FLOW CHARACTERISTICS ANALYSIS OF A TWO-PHASE SUSPENSION BETWEEN ROTATING POROUS CYLINDERS WITH RADIAL AND AXIAL FLOWS

by

Yu-Chuan ZHU[a], Qing-He XIAO[a], Ming-Xin GAO[a], Qian LIU[a] and Zhanhong WAN[b,c*]

[a] Engineering Training Center, University of Science and Technology Liaoning, Anshan, China
[b] Ocean College, Zhejiang University, Hangzhou, China
[c] State Key Laboratory of Satellite Ocean Environment Dynamics, Hangzhou, China

Original scientific paper
https://doi.org/10.2298/TSCI1804857Z

The flow characteristics problem of the two-phase suspension in the design of filters is presented, and the hydrodynamic stability is carried out to study the flow characteristics of a two-phase suspension between a rotating porous inner cylinder and a concentric, stationary, porous outer cylinder when radial flow and axial flow are present. Linear stability analysis results in an eigenvalue problem that is solved numerically by Wan's method. The results reveal that the critical Taylor number for the onset of instability is altered by other parameters. For given correlation parameters, increasing the axial Reynolds number increases the critical Taylor number for transition very slightly, the critical Taylor number decreases as the axial Reynolds number becomes negative.

Key words: *two-phase suspension, critical Taylor number, hydrodynamic stability, axial and radial Reynolds number*

Introduction

The flow characteristics of a two-phase suspension between rotating porous cylinders has been researched in theoretical and experimental standpoints. This paper focuses on the linear stability of a two-phase suspension between a rotating porous inner cylinder and a concentric, stationary, porous outer cylinder when radial flow and axial flow are present. Taylor [1] researched the flow stability of a viscous liquid between two rotating cylinders through a simple flow visualization experiment, the onset of the instability was found in this flow at first. After the Taylor's pioneering work Chandrasekhar [2] found the onset of instability under a variety of externally impressed conditions. Kataoka [3] researched Taylor vortices and instabilities in circular Couette flows. He found that the stability of Taylor vortex flow is altered when some complex conditions is added to the flow system. Some researchers [4-6] found that an axial flow affects the stability of the Taylor vortex. Likewise, when a radial flow is present in the flow between rotating porous cylinders, the stability of the Taylor vortex would be altered [7, 8].

Nearly researches on the stability of circular Couette flow had been done for simple Newtonian fluids. They came up with a few notable results about this. For example, Khayat

* Corresponding author, e-mail: wanzhanhong@zju.edu.cn

[9] found that the fluid elasticity also affects the stability of the viscoelastic fluids. However, experimental results indicate the stability of the viscoelastic fluids depending upon the polymer solution used [10]. The stability of viscous flow between rotating porous cylinders with radial flow was researched by Min *et al.* [11]. They provided that radially inward flow and strong outward flow have a stabilizing effect, while weak outward flow has a destabilizing effect on the Taylor vortex instability. By solving the Navier-Stokes and continuity equations, Johnson *et al.* [12] found that both radial inflow and outflow affect the critical Taylor number, they also found that increasing the axial Reynolds number increases the critical Taylor number for transition very slightly with a given radial Reynolds number. Ali *et al.* [13] researched the hydrodynamic stability of a suspension in cylindrical Couette flow at given different parameters. However, his research is incompleteness, he ignored the axial flow's effect. In my recent research, some works have been done about the stability of a two-phase suspension between the rotating cylinders at given different parameters, when the radial flow and the axial flow are added to this flow.

Based on the methodology of stability analysis for suspension flows established in earlier works for different flow fields, such as channel flow [14-16], pipe flow [17], and Taylor-Couette flow [18], in the present study, we provide a numerical method of the linear hydrodynamic stability analysis for the two-phase flow in annulus between a rotating inner cylinder and fixed concentric outer cylinder. The suspended particles are treated as the continuous phase. The critical Taylor number is an important parameter for the transition from stable circular flow to supercritical Taylor vortex flow, it is obtained under all given conditions. The relationship between the critical Taylor number and the other parameters is discovered.

Problem formulation and stability analysis

In this case, the continuity and Navier-Stokes equations in cylindrical co-ordinates (r, θ, z) are applied to the continuous fluid phase and the discontinuous particle phase. The flow is assumed to be steady and the fluid is incompressible. The cylinders are assumed to be infinitely long with the inner cylinder rotating and the outer cylinder fixed. The velocity field (U, V, W) is:

$$\overline{U}(r)^* = \frac{u_1 r_1}{r} = \frac{\alpha\nu}{r^*} \tag{1a}$$

$$\overline{V}(r)^* = H_1 r^{*\alpha+1} + H_2 \frac{1}{r^*} \tag{1b}$$

$$\overline{W}_0(r)^* = \beta\frac{\nu}{d}C_0\left[\left(\frac{r}{d}\right)^2 + D_0\ln\left(\frac{r}{d}\right) + E_0\right], \qquad \text{for } \alpha = 0 \tag{1c}$$

$$\overline{W}_1(r)^* = \beta\frac{\nu}{d}C_1\left[\left(\frac{r}{d}\right)^2 + D_1\ln\left(\frac{r}{d}\right) + E_1\right], \qquad \text{for } \alpha \neq 0 \tag{1d}$$

Here, $\alpha = u_1 r_1/\nu$ is the radial Reynolds number and $\beta = \overline{w}d/\nu$ – the axial Reynolds number, where u_1 is the radial velocity through the wall of the inner porous cylinder with a negative value when inward from the axis of rotation, r_1 – the inner radius of the cylinder, $\overline{w}$ – the average axial velocity, $d = r_2 - r_1$ – the gap between the cylinders, and ν – the kinematic viscosity. The coefficients H_1, H_2, C_0, D_0, E_0, C_1, D_1, and E_1 are:

$$H_1 = \frac{-\Omega_1 \eta^2}{r_2^{\alpha}(1-\eta^{\alpha+2})}, \qquad H_2 = \frac{r_1^2 \Omega_1}{1-\eta^{\alpha+2}},$$

$$C_0 = \frac{-2}{1+\frac{1}{1-\eta}\left(\frac{2\eta}{1-\eta}+\frac{1+\eta}{\ln\eta}\right)}, \qquad D_0 = \frac{1+\eta}{1-\eta}\frac{1}{\ln\eta}, \qquad E_0 = \frac{1+\eta}{1-\eta}\frac{\ln(1-\eta)}{\ln\eta} - \frac{1}{(1-\eta)^2},$$

$$C_1 = \frac{2(2+\alpha)(\eta^{\alpha}-1)(1-\eta)^2}{(2-\alpha)(1-\eta^{\alpha+2})+(2+\alpha)(\eta^2-\eta^{\alpha})}, \qquad D_1 = \frac{(1-\eta^2)(1-\eta)^{\alpha-2}}{\eta^{\alpha}-1}, \qquad E_1 = \frac{\eta^2-\eta^{\alpha}}{(\eta^{\alpha}-1)(1-\eta)^2}$$

where $\eta = r_1/r_2$ is the radius ratio, Ω_1 and Ω_2 are the inner and outer angular velocity. For axisymmetric flow, the continuity and Navier-Stokes equations for the fluid phase are:

$$\frac{\partial V_{\mathrm{fr}}^*}{\partial r^*} + \frac{1}{r^*}\frac{\partial V_{\mathrm{f}\theta}^*}{\partial \theta^*} + \frac{\partial V_{\mathrm{fz}}^*}{\partial z^*} + \frac{V_{\mathrm{fr}}^*}{r^*} = 0 \tag{2a}$$

$$\frac{\partial V_{\mathrm{fr}}^*}{\partial t^*} + V_{\mathrm{fr}}^*\frac{\partial V_{\mathrm{fr}}^*}{\partial r^*} + \frac{V_{\mathrm{f}\theta}^*}{r^*}\frac{\partial V_{\mathrm{fr}}^*}{\partial \theta^*} + V_{\mathrm{fz}}^*\frac{\partial V_{\mathrm{fr}}^*}{\partial z^*} - \frac{V_{\mathrm{f}\theta}^{*2}}{r^*} =$$

$$= \nu\left(\frac{\partial^2 V_{\mathrm{fr}}^*}{\partial r^{*2}} + \frac{1}{r^*}\frac{\partial V_{\mathrm{fr}}^*}{\partial r^*} + \frac{1}{r^{*2}}\frac{\partial^2 V_{\mathrm{fr}}^*}{\partial \theta^{*2}} + \frac{\partial^2 V_{\mathrm{fr}}^*}{\partial z^{*2}} - \frac{2}{r^{*2}}\frac{\partial V_{\mathrm{f}\theta}^*}{\partial \theta^*} - \frac{V_{\mathrm{fr}}^*}{r^{*2}}\right) - \frac{1}{\rho_{\mathrm{f}}}\frac{\partial p^*}{\partial r^*} - \frac{nF_r^*}{\rho_{\mathrm{f}}} \tag{2b}$$

$$\frac{\partial V_{\mathrm{f}\theta}^*}{\partial t^*} + V_{\mathrm{fr}}^*\frac{\partial V_{\mathrm{f}\theta}^*}{\partial r^*} + \frac{V_{\mathrm{f}\theta}^*}{r^*}\frac{\partial V_{\mathrm{f}\theta}^*}{\partial \theta^*} + V_{\mathrm{fz}}^*\frac{\partial V_{\mathrm{f}\theta}^*}{\partial z^*} + \frac{V_{\mathrm{fr}}^* V_{\mathrm{f}\theta}^*}{r^*} = \nu\left(\frac{\partial^2 V_{\mathrm{f}\theta}^*}{\partial r^{*2}} + \frac{1}{r^*}\frac{\partial V_{\mathrm{f}\theta}^*}{\partial r^*} + \right.$$

$$\left. + \frac{1}{r^{*2}}\frac{\partial^2 V_{\mathrm{f}\theta}^*}{\partial \theta^{*2}} + \frac{\partial^2 V_{\mathrm{f}\theta}^*}{\partial z^{*2}} - \frac{V_{\mathrm{f}\theta}^*}{r^{*2}} + \frac{2}{r^{*2}}\frac{\partial V_{\mathrm{fr}}^*}{\partial \theta^*}\right) - \frac{1}{r^*}\frac{\partial p^*}{\partial \theta^*} - \frac{nF_\theta^*}{\rho_{\mathrm{f}}} \tag{2c}$$

$$\frac{\partial V_{\mathrm{fz}}^*}{\partial t^*} + V_{\mathrm{fr}}^*\frac{\partial V_{\mathrm{fz}}^*}{\partial r^*} + \frac{V_{\mathrm{f}\theta}^*}{r^*}\frac{\partial V_{\mathrm{fz}}^*}{\partial \theta^*} + V_{\mathrm{fz}}^*\frac{\partial V_{\mathrm{fz}}^*}{\partial z^*} =$$

$$= \nu\left(\frac{\partial^2 V_{\mathrm{fz}}^*}{\partial r^{*2}} + \frac{1}{r^*}\frac{\partial V_{\mathrm{fz}}^*}{\partial r^*} + \frac{1}{r^{*2}}\frac{\partial^2 V_{\mathrm{fz}}^*}{\partial \theta^{*2}} + \frac{\partial^2 V_{\mathrm{fz}}^*}{\partial z^{*2}}\right) - \frac{1}{\rho_{\mathrm{f}}}\frac{\partial p^*}{\partial z^*} - \mathrm{g} - \frac{nF_z^*}{\rho_{\mathrm{f}}} \tag{2d}$$

In eqs. (2a)-(2d), the asterisks indicate dimensional variables, and (V_{fr}^*, $V_{\mathrm{f}\theta}^*$, V_{fz}^*) are the flow velocities in the r^*, θ^*, and z^* directions, respectively. The t^* is the time, p^* – the pressure, ρ_{f} – the fluid density, n – the number density of the particle, and g – the acceleration of gravity. The continuity and Navier-Stokes equations for the particulate phase are:

$$\frac{\partial \alpha_{\mathrm{p}}}{\partial t^*} + \frac{\partial V_{\mathrm{pr}}^* \alpha_{\mathrm{p}}}{\partial r^*} + \frac{1}{r^*}\frac{\partial V_{\mathrm{p}\theta}^* \alpha_{\mathrm{p}}}{\partial \theta^*} + \frac{\partial V_{\mathrm{pz}}^* \alpha_{\mathrm{p}}}{\partial Z^*} + \frac{\alpha_{\mathrm{p}} V_{\mathrm{pr}}^*}{r^*} = 0 \tag{3a}$$

$$\frac{\partial V_{\mathrm{pr}}^*}{\partial t^*} + V_{\mathrm{pr}}^*\frac{\partial V_{\mathrm{pr}}^*}{\partial r^*} + \frac{V_{\mathrm{p}\theta}^*}{r^*}\frac{\partial V_{\mathrm{pr}}^*}{\partial \theta^*} + V_{\mathrm{pz}}^*\frac{\partial V_{\mathrm{pr}}^*}{\partial z^*} - \frac{V_{\mathrm{p}\theta}^{*2}}{r^*} = -\frac{1}{\rho_{\mathrm{p}}}\frac{\partial p^*}{\partial r^*} + \frac{nF_r^*}{\alpha_{\mathrm{p}}\rho_{\mathrm{p}}} \tag{3b}$$

$$\frac{\partial V_{p\theta}^{*}}{\partial t^{*}} + V_{pr}^{*}\frac{\partial V_{p\theta}^{*}}{\partial r^{*}} + \frac{V_{p\theta}^{*}}{r^{*}}\frac{\partial V_{p\theta}^{*}}{\partial \theta^{*}} + V_{pz}^{*}\frac{\partial V_{p\theta}^{*}}{\partial z^{*}} + \frac{V_{pr}^{*}V_{p\theta}^{*}}{r^{*}} = -\frac{1}{r^{*}\rho_{p}}\frac{\partial p^{*}}{\partial \theta^{*}} + \frac{nF_{\theta}^{*}}{\alpha_{p}\rho_{p}} \tag{3c}$$

$$\frac{\partial V_{pz}^{*}}{\partial t^{*}} + V_{pr}^{*}\frac{\partial V_{pz}^{*}}{\partial r^{*}} + \frac{V_{p\theta}^{*}}{r^{*}}\frac{\partial V_{pz}^{*}}{\partial \theta^{*}} + V_{pz}^{*}\frac{\partial V_{pz}^{*}}{\partial z^{*}} = -\frac{1}{\rho_{p}}\frac{\partial p^{*}}{\partial z^{*}} - g + \frac{nF_{z}^{*}}{\alpha_{p}\rho_{p}} \tag{3d}$$

In eqs. (3a)-(3d), (V_{pr}*, $V_{p\theta}$*, V_{pz}*) are the particle velocities in the r*, θ* and z* directions, ρ_p – the particle density, α_p – the volume fraction of particles, and α_f – the volume fraction of the fluid such that $\alpha_p + \alpha_f = 1$. However, we should note that the volume fraction of particles is related to the number density by $\alpha_P = n\pi\phi^{*3}/6$, where ϕ* is the diameter of the particle. The F* on the right-hand side of the momentum phase equation is the Stokes drag and added mass, expressed:

$$F_i^{*} = 3\pi\mu\phi^{*}(V_{fi}^{*} - V_{pi}^{*}) + \frac{\rho_f \pi(\phi^{*})^3}{12}\frac{\partial}{\partial t^{*}}(V_{fi}^{*} - V_{pi}^{*}) \quad \text{for} \quad i = r, \theta, z \tag{4}$$

In the dimensionless form of the continuity and Navier-Stokes equations the following parameters will appear: the density ratio $\varepsilon = \rho_p/\rho_f$ and the Taylor number $\mathrm{Ta} = \Omega_1 r_1 d/\nu$. Separation of the average values of variables and perturbation components is used in the linear stability analysis such that:

$$\begin{aligned} V_{fr}^{*} &= \overline{U}(r)^{*} + u'(r,z,\theta,t)^{*} & V_{pr}^{*} &= \overline{U}(r)^{*} + u_p'(r,z,\theta,t)^{*} \\ V_{f\theta}^{*} &= \overline{V}(r)^{*} + v'(r,z,\theta,t)^{*}, & V_{p\theta}^{*} &= \overline{V}(r)^{*} + v_p'(r,z,\theta,t)^{*}, \\ V_{fz}^{*} &= \overline{W}(r)^{*} + w'(r,z,\theta,t)^{*} & V_{pz}^{*} &= \overline{W}(r)^{*} + w_p'(r,z,\theta,t)^{*} \end{aligned} \qquad \begin{aligned} p^{*} &= P^{*} + p'(r,z,\theta,t)^{*} \\ \alpha_p^{*} &= A^{*} + a_p'(r,z,\theta,t)^{*} \end{aligned} \tag{5}$$

The perturbations are expressed:

$$\frac{u'}{u(r)} = \frac{v'}{v(r)} = \frac{w'}{w(r)} = e^{[\sigma t + i(kz + m\theta)]}, \quad \frac{u_p'}{u_p(r)} = \frac{v_p'}{v_p(r)} = \frac{w_p'}{w_p(r)} = e^{[\sigma t + i(kz + m\theta)]}$$

$$\frac{p'}{\omega(r)} = e^{[\sigma t + i(kz + m\theta)]}, \quad \frac{a_p'}{a_p(r)} = e^{[\sigma t + i(kz + m\theta)]} \tag{6}$$

where $u(r)$, $v(r)$, $w(r)$, $u_p(r)$, $v_p(r)$, $w_p(r)$, $\omega(r)$, and $\alpha_p(r)$ are the amplitudes of the disturbance, k – the axial wave number of the disturbance, m – the circumferential direction wave number of the disturbance, and σ – an amplification factor.

Equations (1), (4), (5), and (6) are substituted into dimensionless continuity and Navier-Stokes equations. Linearization of the equations by discarding higher order non-linear terms result in the final form of the disturbance equations.

The result of the continuity and Navier-Stokes equations for the two-phase fluid is obtained by a solution procedure. The eigenvalue problem can be rearranged and written in the implicit functional form:

$$\mathrm{H}U = \sigma \mathrm{K}U \tag{7}$$

where H and K are two matrices which are made from the coefficients of the equations. The solution to eigenvalue problem is obtained by spectral methods using the procedure outlined in Wan *et al* [19, 20]. We seek to find the stability conditions as the amplification factor σ is set to zero. The relationships between the other parameters in this flow were worked out.

Results and discussion

The critical Taylor number is an important parameter for the transition from stable circular flow to supercritical Taylor vortex flow. Its value becomes a standard of the flow stability of the two-phase suspension between rotating porous cylinders. We found that the parameters A, η, ϕ, ε, α, β, m, and k have some effects on the critical Taylor number.

As the particle concentration ranged from 0.01 to 0.07, the critical Taylor number for transition from stable cylindrical flow to supercritical Taylor vortex flow for the two-phase fluid is shown in fig. 1 for three radius ratios. As the radius ratios increases, the two-phase fluid becomes more stable. The stability effect is even more striking for the smaller gap (η = 0.95). The critical Taylor number decreases by about 10% as the particle concentration increases from 0.01 to the maximum concentration. Decreasing the particle concentration can make the two-phase suspension more stability. At the same time, the axial flow affects the stability of this fluid is also evident in fig.1. Increasing the axial Reynolds number increases the stability of the flow, although the effect is small over the range of the particle concentration.

The range of particle diameters that was considered is consistent with physically realizable systems. Particle diameters to gap widths ranged from 0.001 mm to 0.005 mm. The effect of the diameter on the critical Taylor number is shown in fig. 2. The critical Taylor number obviously decreases, as the diameter increases from 0.001 mm to 0.005 mm. The critical Taylor number decreases by about 40% as the particle diameter increases from 0.001 mm to the maximum concentration. The destabilizing effect is very striking for increasing the diameter. Likewise, the effect of the axial Reynolds number is also recorded in fig. 2. The critical Taylor numbers for β = 10 and β = –10 is very different. The critical Taylor number increases for β = 10, but decreases for β = –10.

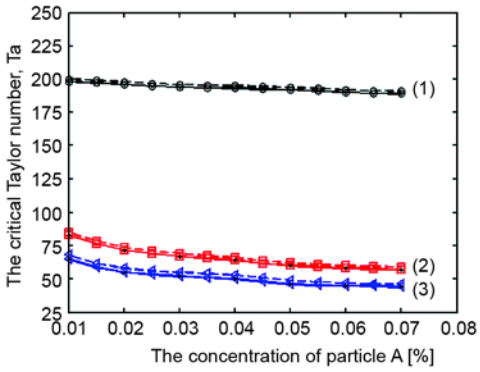

Figure 1. Critical Taylor number for several radius ratios as a function of particle concentration A for the two-phase suspension; (1) β = 0 (no axial flow), solid curves; (2) β = 10, dashed curves; η = 0.95, η = 0.75; η = 0.45; (3) (ε = 1, ϕ = 0.004, m = 0, k = 3.13, α = 0)

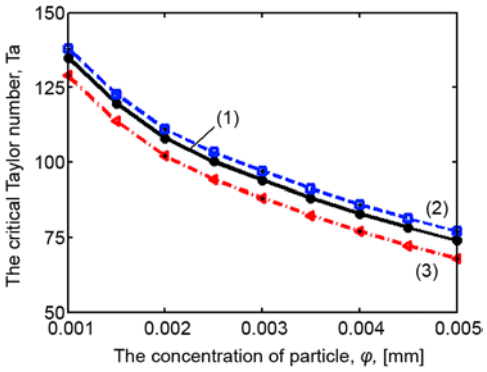

Figure 2. The effect of the particle diameter on the critical Taylor number; (1) β = 0 (no axial flow), solid curves; (2) β = 10, dashed curves; (3) β = –10, dot-dash curves. (ε = 1, m = 0, k = 3.13, α = 0, A = 0.01, η = 0.75)

Particle density ratio was used that are inconsistent with different heavy particles in this fluid. The critical Taylor number is shown in fig. 3 with the density ratio ranging from 1 to 20. As the density ratio increases from 1 to 5, the decrease in the critical Taylor number is very striking. The density ratios ranging from 5 to 10 have little effect in the critical Taylor number. But the density ratio increases from 10 to 15, the critical Taylor number decreases to only a small fraction. When the density ratio varies from 15 to 20, the decrease in the critical Taylor number is negligible. Likewise, the axial flow affects the stability of this fluid is also evident in fig. 3. The two-phase suspension is more stability for $\beta = 10$, but more instability for $\beta = -10$.

The effect of the radial Reynolds number on the critical Taylor number is shown in fig. 4 with axial Reynolds numbers ranging from –5 to 5. When the radial Reynolds number is closed to zero, the critical Taylor number obviously decreases. However, the larger negative or positive radial flow the opposite situation occurs. We also consider the axial Reynolds number affect the stability of this system. The critical Taylor number increases, when the axial Reynolds number is equal to 10. But decreases for axial Reynolds number being equal to –10. Increasing the critical Taylor number for the onset of instability indicates a stabilizing effect. As the direction of the axial flow is down, the flow is more instability.

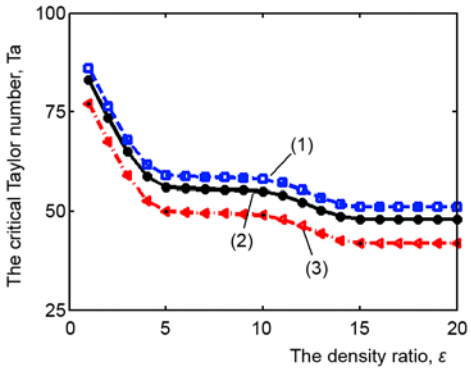

Figure 3. The effect of the density ratio on the critical Taylor number; (1) $\beta = 10$ dashed curves; (2) $\beta = 0$ (no axial flow), solid curves; (3) $\beta = -10$, dot-dash curves. ($\phi = 0.001$, $m = 0$, $\eta = 0.75$, $k = 3.13$, $\alpha = 0$, $A = 0.01$)

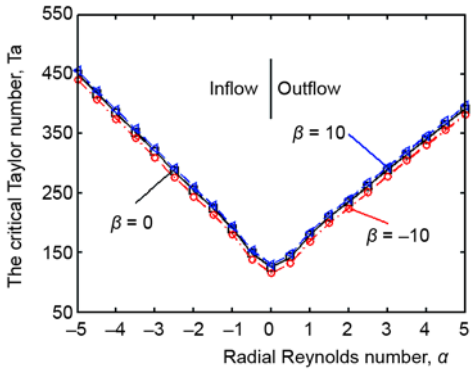

Figure 4. The effect of the radial Reynolds number on the critical Taylor number; $\beta = 0$ (no axial flow), solid curves; $\beta = 10$, dashed curves; $\beta = -10$, dot-dash curves. ($\varepsilon = 1$, $m = 0$, $k = 3.13$, $\phi = 0.001$, $A = 0.01$, $\eta = 0.75$)

Conclusions

The result of the flow characteristics of the suspension between rotating porous cylinders indicate that radial flow and axial flow have an obviously influence. Before this research many works had been done about the stability of viscous flow between rotating porous with radial flow and axial flow, they did not consider the viscous flow was a two-phase flow. In the pioneering work a lot of researchers only considered the axial wave number's effect. Their results are not complete. However, our results with considering the factors completely make the analysis of the flow characteristics more trustworthy.

There are many parameters effecting on the flow characteristics analysis of the two-phase flow between a rotating porous inner cylinder and a concentric, stationary, porous outer cylinder. We mainly considered the concentration of particle, A, the diameter of particle, ϕ,

the density ratio, ε, the radial Reynolds number, α, and the axial Reynolds number, β, have some effects on this system. At first as the gap between rotating cylinders changes to be larger, the flow becomes less stable. At second the critical Taylor number obviously decreases with the diameter of particle increasing. At third varying the stability of the two-phase suspension is negligible or striking, as the density ratio increases from 1 to 20. At least the strong radial inflow or outflow's effect is different with the weak radial inflow or outflow's effect in this system, the strong radial flow makes the flow more stability. However, when the axial flow is a strong down flow, the critical Taylor number increases, the axial flow makes this system more stability. Our results suggest an estimate of the conditions for the two-phase suspension to become unstable, when radial flow and axial flow are present in this system.

Acknowledgment

This work is supported by the National Natural Science Foundation of China (Grant No. 11572283, 11602179), the Education Department Foundation of Liaoning Province (Grant No. 2017LNQN08), and the Youth Foundation of Science and Technology Liaoning University (Grant No. 2016QN04).

References

[1] Taylor, G. I., Stability of A Viscous Liquid Contained Between Two Rotating Cylinders, *Philos. Trans.R. Soc. London, Ser. A, 1* (1923), Jan., pp. 223-289
[2] Chandrasekhar, S., *Hydrodynamic and Hydromagnetic Stability*, Oxford University Press, Oxford, UK, 1961
[3] Kataoka, K., Taylor Vortices and Instabilities In Circular Couette Flows, *in: Encyclopedia of Fluid Mechanics* (Ed. N. P. Cheremisinoff), Gulf, Houston, Tex., USA, 1986, pp. 236-274
[4] Kaye, J., *et al.*, Modes of Adiabatic and Diabatic Fluid Flow in an Annulus with an Inner Rotating Cylinder, *Trans. ASME 80* (1958), pp. 753-765
[5] Chandrasekhar, S., The Hydrodynamic Stability of Viscid Flow between Coaxial Cylinders, *Proc. Natl. A cad. Sci. U.S.A. 46* (1960), 1, pp. 141-143
[6] DiPrima, R. C., The Stability of a Viscous Fluid between Rotating Cylinders with an Axial Flow, *J. Fluid Mesh, 9* (1960), 4, pp. 621-631
[7] Bahl, S. K., Stability of Viscous Flow between Two Concentric Rotating Porous Cylinders, *Def. Sci. J., 25* (2014), 4, pp. 139-144
[8] Buhler, K., Taylor Vortex Flow with Superimposed Radial Mass Flux, *in Ordered and Turbulent Patterns in Taylor-Couette Flow, 297* (1992), pp. 197-203
[9] Khayat, R. E., Onset of Taylor Vortices and Chaos in Viscoelastic Fluids, *Phys. Fluid, 7* (1995), 9, pp. 2191-2219
[10] Yi, M. K., *et al.*, Experimental Studies on the Taylor Instability of Dilute Polymer Solutions, *J. Non-Newtonian Fluid Mesh, 72* (1997), 2-3, pp. 113-139
[11] Min, K., *et al.*, Hydrodynamic Stability of Viscous Flow between Rotating Porous Cylinders with Radial Flow, *Phys. Fluids, 6* (1994), 1, pp. 144-161
[12] Johnson, E. C., *et al.*, Hydrodynamic Stability of Flow between Rotating Porous Cylinders with Radial and Axial Flow, *Phys. Fluids, 9* (1997), 12, pp. 3687-3696
[13] Ali, M. E., *et al.*, Hydrodynamic Stability of a Suspension in Cylindrical Couette Flow, Phys. Fluids, *14* (2002), 3, pp. 1253-1254
[14] Lin, J., *et al.*, Stability in Channel Flow with Fiber Suspensions, *Progress in Natural Science, 13* (2003), 2, pp. 95-99
[15] You, Z., *et al*, Stability and Drag Reduction in Transient Channel Flow of Fiber Suspensions, *Chinese Journal of Chemical Engineering, 12* (2004), 3, pp. 319-323
[16] You, Z., *et al.*, Effects of Tensor Closure Models and 3-D Orientation on the Stability of Fiber Suspensions in a Channel Flow, *Applied Mathematics and Mechanics, 26* (2005), 3, pp. 307-312
[17] You, Z., *et al.*, Stability in the Circular Pipe Flow of Fiber Suspensions, *Journal of Hydrodynamics, Ser. B, 15* (2003), 2, pp. 12-18

[18] Wan, Z., *et al*, Research on the Specific Viscosity of Semi-Concentrated Fiber Suspensions, *Modern Physics Letters B, 22* (2008), 29, pp. 2857-2868
[19] Wan, Z., *et al.*, The Effects of Closure Model of Fiber Orientation Tensor on the Instability of Fiber Suspensions in the Taylor-Couette Flow, *Modern Physics Letters B, 21* (2007), 24, pp. 1611-1625
[20] Wan, Z., *et al.*, Dynamic Stability of Non-Dilute Fiber Shear Suspensions, *Thermal Science, 16* (2012), 5, pp. 1551-1555

Paper submitted: March 23, 2017
Paper revised: September 24, 2017
Paper accepted: September 24, 2017